Microwave surface impedance measurements of Sr_2RuO_4: The effect of impurities

P. J. Baker, R. J. Ormeno, and C. E. Gough
School of Physics and Astronomy, University of Birmingham, Edgbaston, Birmingham B15 2TT, United Kingdom

Z. Q. Mao, S. Nishizaki, and Y. Maeno
Department of Physics, Kyoto University, Kyoto 606-01, Japan
and CREST, Japan Science and Technology Corporation, Kawaguchi, Saitama 332-0012, Japan

(Received 18 May 2009; revised manuscript received 29 July 2009; published 29 September 2009)

The temperature, purity, and frequency dependence of the real and imaginary components of the complex surface impedance of three single crystals of the proposed *p*-wave superconductor Sr_2RuO_4, with T_c values of 1.40, 1.24, and 0.74 K, have been measured over a range of microwave frequencies from 4–16 GHz down to 100 mK. The unusual superconducting microwave properties can be described by a multiband, two-fluid model consistent with electron relaxation times remaining largely unchanged on entering the superconducting state and energy gaps on all bands having the same temperature dependence. In addition, the model is consistent with nonmagnetic impurity scattering strongly suppressing the superconducting fractions leading to large residual losses at low temperatures and an increase in penetration depth. Model independent derivations of the complex microwave conductivity are shown to be largely consistent with such a scenario.

DOI: 10.1103/PhysRevB.80.115126 PACS number(s): 74.25.Fy, 78.70.Gq, 74.70.Pq

I. INTRODUCTION

The superconductor Sr_2RuO_4 has attracted a considerable amount of interest[1] since its discovery in 1994.[2] As well as being the only known layered-perovskite superconductor without copper, there is substantial evidence that Sr_2RuO_4 is a triplet *p*-wave superconductor.[3] However, the symmetry of the superconducting gap on the three contributing conduction bands remains a topic of considerable current interest.[4,5] Arguments have been made for a gapless chiral dependence with a nodeless chiral state of the type $d(k)=\Delta_0\hat{z}(\sin k_x+i \sin k_y)$ on the γ band, assumed to be largely responsible for superconductivity, with line nodes along the z direction on the α and β bands. Support for such a model is provided by the heat-capacity measurements of Deguchi *et al.*,[6] consistent with microscopic calculations with contributions from all three bands by Nomura and Yamada.[7]

Early signs for unconventional superconductivity in Sr_2RuO_4 came from data showing an extreme sensitivity of T_c on nonmagnetic impurities and defects.[8,9] T_c is dramatically reduced by increases in the residual dc resistivity ρ_0 of only tenths of $\mu\Omega$ cm. The depression of T_c can be described by Abrikosov-Gorkov theory for nonmagnetic pair breaking impurities in an anisotropic superconductor.[10] Specific-heat measurements on samples of various purity[11] indicate the presence of a residual density of states (RDOS) in the superconducting state at 0 K. RDOS tends to zero in the ultraclean limit suggesting that it is a defect and/or impurity induced effect. A similar behavior has been observed in NMR measurements.[12,13]

Here we present microwave surface impedance measurements on three samples of Sr_2RuO_4 of varying purity, with $T_cs \sim 1.40$, 1.24, and 0.74 K, from which we are able to extract the frequency and purity dependence of the real and imaginary parts of the microwave conductivity. Previous microwave measurements on very pure samples of Sr_2RuO_4 ($T_c \sim 1.47$ K) by Ormeno *et al.*[14] were interpreted in terms of a residual fraction of charge carriers remaining unpaired. Such charge carriers at low temperature could account for losses at low temperature that were a significant faction of those in the normal state—defined here as the residual microwave normal fraction (RMNF). This will not in general be the same as the RDOS derived from heat-capacity measurements as microwave measurements also involve quasiparticle life times.

In the first part of the paper, we show that the unusual temperature, frequency, and purity dependence of the complex microwave surface impedance can be described by a multiband, two-fluid model based on the following assumptions: (a) a common quasiparticle mean–free-path ℓ on all bands, (b) a common temperature dependent superconducting fraction $f(T)$ on each band, consistent with superconductivity in the α and β bands being driven by superconductivity on the γ band and (c) impurity scattering causing a fraction of charge carriers in each band to remain normal. In the second part, the complex microwave conductivity is derived directly from the real and imaginary components of the complex microwave surface impedance. The temperature, frequency, and purity dependence of the derived microwave conductivity is shown to be consistent with the above assumptions. In particular, the imaginary part of the derived conductivity gives a penetration depth that increasing markedly with impurity scattering, consistent with the depairing of electrons by nonmagnetic impurities. There is no marked change in the real part of the microwave conductivity on entering the superconducting state, implying a quasiparticle relaxation rate that is little changed from its normal state value on entering the superconducting state, in marked contrast to conventional *s* and *d* wave superconductors.[15]

Although microwave measurements cannot provide any direct evidence on the symmetry of the gap parameters on the three contributing bands, any successful microscopic theory for the electrodynamic response must ultimately describe the purity, temperature, and frequency dependence observed in these measurements.

II. MICROWAVE MEASUREMENTS

The samples used in these experiments were grown by the floating zone method in Y. Maeno's group in Kyoto. Electron probe microanalysis (EMPA) scans by Mackenzie *et al.*[8] on very similar crystals to those used here showed that the impurities present were nonmagnetic elements Al, Si, Ba, and Ca. The platelike crystals had typical dimensions of $\sim 1 \times 1 \times 0.03$ mm^3, with the c axis perpendicular to the major faces.

Because microwave measurements are sensitive to surface defects, all samples were etched in an ethanol-bromine solution prior to making measurements.

A cavity perturbation technique[16] was used to measure the complex surface impedance $Z_s = R_s + iX_s$, where R_s and X_s are the surface resistance and reactance, respectively. Measurements on each sample were taken at 4.5 GHz in an ^{3}He system down to ~ 300 mK and at 10.7 and 15.2 GHz in an adiabatic demagnetization refrigeration (ADR) system down ~ 100 mK. Individual samples were glued to the end of a sapphire rod and positioned at the center of a high Q ($\approx 10^5$) dielectric resonator using TE_{01n} modes. For all modes, the quasihomogenous microwave magnetic field was perpendicular to the major faces of the sample, confining the currents to the ab plane. A hot-finger technique[17] was used to raise and control the temperature of the sapphire rod supporting the sample to temperatures up to ~ 30 K.

Small changes in the resonant frequency $f_0(T)$ and bandwidth $f_b(T)$ were measured, from which $R_s(T)$ and $\Delta X_s(T)$ were derived using the perturbation formulas $R_s(T) + i\Delta X_s(T) = \Gamma[f_b(T) - 2i\Delta f_0(T)]$, where Γ is the geometrical factor determined by the microwave field at the sample location. Accurate measurements of $\Delta X_s(T)$ were achieved by making all measurements relative to a specific fixed temperature, thus overcoming the unavoidable problem of long term drifts in such measurements. The temperature dependence of the empty cavity bandwidth and frequency shifts were measured separately and subtracted from the sample measurements. The Γ factor was determined indirectly by fitting the normal state f_b data to the R_s values predicted from dc measurements, see Sec. II A.

At low temperature and high input powers sample heating can be important. Measurements were therefore made using input powers well below the input power where sample heating was first observed. At higher temperatures, the measurements were reproducible up to the highest input powers available (1 mW).

The measurement technique was tested on a Nb sample of similar dimension. The results were consistent with BCS theory, giving an exponential temperature dependence of both R_s and X_s at low temperature, with $f_b(T \to 0)$ falling to the measured cavity background value. This gave us confidence in interpreting the resistive and reactive components of the surface impedance as sample induced rather than background artifacts.

A. Surface Impedance

The surface impedance in the local limit is given by

$$Z_s(T) = \sqrt{\frac{i\omega\mu_0}{\sigma}}, \tag{1}$$

where the angular frequency $\omega = 2\pi f_0$ and σ is the conductivity.

In the normal state, we assume a Drude model, $\sigma = [\rho(1 + i\omega\tau)]^{-1}$, where ρ is the dc conductivity and τ is the mean scattering time of the charge carriers. In $SrRuO_4$ the purity is such that the normal state $\omega\tau$ term is significant at microwave frequencies, so that changes in conductivity on entering the superconducting state are sensitive to the lifetime of thermally excited quasiparticles.

In the ab plane, dc measurements[18] give the Fermi-liquid dependence $\rho(T) = \rho_0 + AT^2$ below $T < 25$ K, with $A = 4.5$–7.3 nΩ cm. For a two-dimensional Fermi metal, the dependence of ρ on the mean-free-path ℓ is given by

$$\rho = \frac{2\pi\hbar d}{e^2 \ell \Sigma_i k_{Fi}}, \tag{2}$$

where d is the interplane separation and k_{Fi} is the wavevector for each of the three bands.[1] In the following analysis, estimates for ρ_0 were made from the observed T_c using previous dc measurements[8] of ρ_0 vs T_c. Assuming ℓ is the same for all charge carriers, the relaxation time τ_i can be calculated for each band using $\tau_i = \ell / v_{Fi}$, where v_F is the Fermi velocity. The band parameters for k_F and v_F were those measured in quantum oscillation experiments.[19]

In the absence of a microscopic model for the electromagnetic properties of a multiband p-wave superconductor, we adopt a two-fluid model approach, used previously to describe the microwave properties of both conventional and cuprate superconductors.[20–22] For a simple two-fluid model, the complex conductivity is given by

$$\sigma_1 - i\sigma_2 = \frac{1}{\rho_0}\left[\frac{1 - f(T)}{1 + i\omega\tau} + \frac{f(T)}{i\omega\tau}\right], \tag{3}$$

where $f(T)$ is the temperature dependence of the superfluid fraction. For a multiband superconductor such as Sr_2RuO_4, with a depairing parameter ε_i depairing a fraction of superconducting charge carriers in each band, the above result can be generalized and combined with the above equations to give a microwave surface impedance

$$Z_s = \sqrt{i\omega\mu_0 \frac{\hbar 2\pi d}{e^2 \ell}} \left(\sum_i k_{Fi} \left\{ (1 - \varepsilon_i) \left[\frac{1 - f(T)}{1 + i\omega\ell / v_{Fi}} + \frac{f(T)}{i\omega\ell / v_{Fi}} \right] + \varepsilon_i \frac{1}{1 + i\omega\ell / v_{Fi}} \right\} \right)^{-1/2}, \tag{4}$$

where the summation is made over each carrier band (i.e., α, β, and γ for Sr_2RuO_4). Electron depairing by impurity or lattice defect scattering leads to significant microwave losses down to the lowest temperatures. The temperature dependence of the complex microwave conductivity is then described by the superconducting fraction $f(T)$ of the remaining charge carriers, which is assumed to be the same for each band, consistent with superconductivity in the γ-band driving superconductivity in the α and β bands.

At low temperatures, $f(T) \rightarrow 1$ and the losses will be determined by the real part of the microwave conductivity, giving a band-averaged ε_{av} defined as the residual microwave normal fraction RMNF

$$\varepsilon_{av} = \mathrm{RMNF} = \frac{\Sigma_i \varepsilon_i n_i / k_{Fi}}{\Sigma_i n_i / k_{Fi}}, \tag{5}$$

where n_i represents the number of contributing charge carriers in each band.

As remarked earlier, the weighted average will not in general be the same as the residual density of states

$$\mathrm{RDOS} = \frac{\Sigma_i \varepsilon_i n_i}{\Sigma_i n_i}. \tag{6}$$

In the following analysis of our measurements, we have to make some simplifications, as there is no way of extracting meaningful information about all three bands of electrons. Two possible scenarios were therefore considered when fitting the measurements using Eq. (4). In the first, we assume that impurity scattering has the same effect on charge carriers in all three bands with a common depairing parameter ε. In the second scenario, we assume that impurity scattering causes preferential depairing on the α and β bands. These bands are treated together with a common depairing parameter $\varepsilon_{\alpha\beta}$, which we increase from $0 \rightarrow 1$ to fit the results to Eq. (4) and increase the depairing parameter ε_γ in the γ band if required. In this scenario, the RMNF is determined by a band-averaged ε_{av} using Eq. (5).

In both scenarios the temperature dependence $f(T)$ was assumed to be the same as that obtained by Bonalde *et al.*[23] using the tunnel-diode technique, see Fig. 4, in close agreement with our earlier microwave measurements on an even purer sample.[14] The scattering time τ in each band was also assumed to be unchanged on entering the superconducting state, again consistent with our previous measurements.

In the second part of the paper, we derive directly the real and imaginary parts of the microwave conductivity from the surface impedance and obtain values for the penetration depth and resistive losses in close agreement with the assumptions made in our empirical model.

B. Complex conductivity and penetration depth

The measurements of R_s and X_s can be converted to σ_1 and σ_2 using

$$\sigma_1(T) = \omega\mu_0 \frac{2R_s(T)X_s(T)}{(R_s(T)^2 + X_s(T)^2)^2} \tag{7}$$

and

$$\sigma_2(T) = \omega\mu_0 \frac{X_s(T)^2 - R_s(T)^2}{(R_s(T)^2 + X_s(T)^2)^2}. \tag{8}$$

Note that the above derivations are very sensitive to the absolute values of $X_s(T)$. This is always a potential problem in microwave measurements, in which only changes in $X_s(T)$ are usually measured, with the absolute values fixed by comparison with predicted normal state values. This can present somewhat uncertain correction factors from finite $\omega\tau$ values and potential nonlocal corrections in pure metals such as $SrRuO_4$. This is why we chose first to describe and analyze our raw data in terms of the surface impedance before extracting the microwave conductivity.

Equation (8) can be used to obtain $f(T) = [\lambda(0)/\lambda(T)]^2$ from

$$\lambda(T) = (\omega\mu_0\sigma_2(T))^{-1/2}. \tag{9}$$

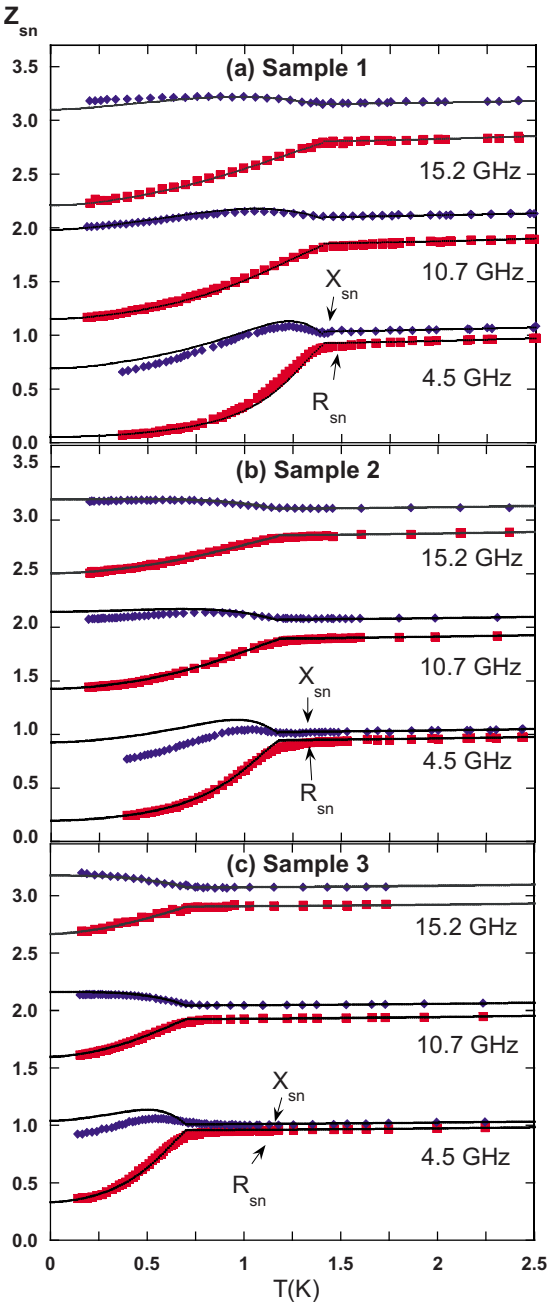

FIG. 1. (Color online) R_{sn} and X_{sn} verses temperature for each sample, normalized at 2.0 K (for clarity the 10.7 and 15.2 GHz plots have been shifted up by +1 and +2, respectively). Normal and superconducting state fits are made using a local Fermi-liquid and two-fluid model, respectively, (see text) with parameters given in Table I.

TABLE I. Input parameters for Z_{sn} fits.

Sample	T_c (K)	ρ_0 ($\mu\Omega$ cm)	First scenario fit	Second scenario fit		
			ε_{av}	$\varepsilon_{\alpha,\beta}$	ε_{γ}	ε_{av}
1	1.4	0.21 ± 0.05	0.42 ± 0.11	0.63 ± 0.17	0	0.28 ± 0.08
2	1.2	0.48 ± 0.05	0.86 ± 0.01	1	0.56 ± 0.03	0.77 ± 0.02
3	0.7	0.72 ± 0.05	0.94 ± 0.01	1	0.80 ± 0.01	0.89 ± 0.01

III. RESULTS AND DISCUSSION

A. Surface Impedance

The measured values for R_{sn} and X_{sn} for each sample are shown in Fig. 1 as a function of temperature. These were normalized to the average of R_s and X_s in the normal state at 2.0 K. The splitting of R_s and X_s in the normal state is a consequence of finite-relaxation times, which for small values of $\omega\tau$ lead to a splitting that increases with both frequency and purity, as illustrated. For clarity, the 10.7 and 15.2 GHz data have been shifted by +1 and +2, respectively.

The solid lines drawn through the experimental data were calculated from Eq. (4) using the first scenario assuming a common depairing factor ε on all three bands. In the second scenario, an almost identical fit could be obtained by assuming that impurity scattering completely suppressed superconductivity in the α and β bands for the less pure samples, with a significant depairing of electrons in the γ band. The fitting parameters for these two scenarios are listed in Table I.

The excellent agreement between the measurements and the prediction of our empirical model [Eq. (4)], particularly at the higher frequencies, supports the assumptions that $f(T)$ and ℓ are the same for all bands. However, there are significant deviations in the measurements of X_s at the lowest frequency for the less pure samples, which may be experimental or arise from some as yet unidentified physical process. Requiring fits to both R_s and X_s at three widely different microwave frequencies using the same set of fitting parameters for a given sample provides a much more demanding test of the proposed model than had R_s alone been measured.

Because the quality of the fits for the two scenarios considered were almost identical, microwave measurements alone cannot be used to distinguish between them. The two scenarios give slightly different values for the total residual microwave normal fractions RMNF=ε and ε_{av} listed in Table I. The RMNFs obtained are also plotted in Fig. 2 for comparison with the residual densities of states derived from heat-capacity measurements.[11]

Referring again to Fig. 1, up to 5 K in the normal state, R_s and X_s both follow the $A+BT^2$ Fermi-liquid temperature dependence observed in dc measurements.[18] The critical temperature marking the transition to the superconducting state is decreased and broadened with increasing impurity, in agreement with dc measurements.[8]

On entering the superconducting state, R_s falls monotonically to nonzero values at low temperatures, reflecting the finite RMNF. In contrast, for all samples, X_s initially increases on entering the superconducting state, with a temperature and frequency dependent peak, which moves to lower temperatures with increasing frequency. As described in our earlier paper[14] on an even purer sample with a slightly higher T_c=1.47 K, the rise and peak in X_s can be described by a conventional two-fluid model with a finite value of $\omega\tau$. As shown in Fig. 1, the data for all three samples, at all frequencies, can be described rather well by Eq. (4), using the values of τ of 6.4, 3.3, and 1.8 ps for samples 1, 2, and 3 deduced from normal-state-resistivity measurements.[8] The fits assume that the quasiparticle lifetimes τ remain unchanged on entering the superconducting state. The near constancy of the *qp* scattering rate in the superconducting state is very different from both *s*- and *d*-wave superconductors[16] and may well be a characteristic signature of *p*-wave superconductivity.

The fits of our measurements to the proposed empirical model are remarkably good, especially to R_s, which is largely responsible for determining the values of ε_{av} in Table I. However, at the lowest frequency, both the predicted height of the peak and low-temperature values for X_s are slightly above the measured values. Small differences are not unexpected in view of the major simplifications presented in our empirical model.

The derived values of RMNF for both scenarios are shown as a function of T_c in Fig. 2 for each sample. Also included are the values obtained by Ormeno *et al.*[14] on a slightly purer sample with $T_c \sim 1.47$ K using a similar

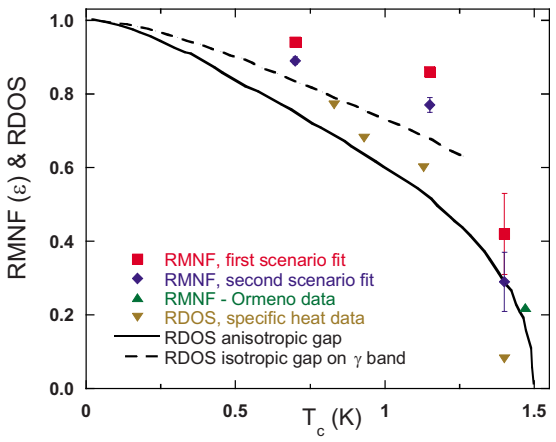

FIG. 2. (Color online) RDOS (normalized by its normal state value) and RMNF data obtained from specific heat (Ref. 11) and R_s measurements respectively, plotted against the T_c of each sample. The RMNF values obtained from both the first and second scenario fitting are shown along with previous data obtained by Ormeno *et al.* (Ref. 14). Also shown are the theoretical predictions for RDOS discussed in the text.

two-fluid model. Plotted on the same axis are the RDOS derived from specific heat measurements[11] and theoretical predictions for a single-band anisotropic gap[24] with $\Delta_{min}/\Delta_{max}=0.25$ (solid line) and a two-fluid model with an isotropic gap confined to the γ band[11] (dashed line).

The RMNF values obtained from both scenarios are in qualitative agreement with, but are somewhat higher than the measured specific-heat RDOS values. The observed increase in RMNF with decreasing purity is confirmed. The microwave estimates for RMNF are in better agreement with RDOS predictions for an isotropic gap primarily on the γ band than with a single anisotropic gap. However, as emphasized earlier, there is no reason to expect RMNF to be the same as RDOS, as the first relates to a thermodynamic property and the second to a transport property involving different Fermi-surface averages.

B. Temperature dependence of $\Delta\lambda$

We assume that in any model the value of $\lambda(0)$ will be frequency independent. This required small corrections to the absolute values of X_s deduced from our earlier fits to the empirical two-fluid model, particularly for the 4.5 GHz measurements, which we have already shown deviate most strongly from the predictions of our empirical model, Eq. (4). Having made the small corrections necessary to ensure that $\lambda(0)$ is frequency independent, we obtain values of $\lambda(0)$ of 1600 ± 50 Å, $3,000\pm50$ Å, and $4,100\pm50$ Å for samples 1, 2, and 3, respectively. The increase in penetration depth with increasing impurity concentration arises from the reduction in number of superconducting electrons from impurity scattering, with an accompanying decrease in T_c from 1.40 to 1.24 K and 0.74 K, respectively.

Figure 3 shows the temperature dependence of $\Delta\lambda=\lambda(T)-\lambda(0)$ plotted against $(T/T_c)^2$ illustrating a nonexponential quadratic temperature dependence at low temperatures, very different from that expected for a fully gapped *s*-wave superconductor.

A quadratic temperature dependence was observed below a crossover temperature T^{cr}, which decreased monotonically with decreasing sample purity. For sample 1, $T^{cr}\sim0.65$ $T_c\sim0.9$ K, in agreement with previous measurements by Ormeno *et al.*[14] and Bonalde *et al.*[23] For samples 2 and 3, $T^{cr}\sim0.55$ $T_c\sim0.63$ K and 0.35 $T_c\sim0.25$ K, respectively. The temperature dependence of $\Delta\lambda$ for sample 3 fits more closely to a T^3 dependence up to ~0.74 $T_c\sim0.52$ K, which is also in agreement with Bonalde's measurements on a sample with $T_c=0.8$ K.

For a clean superconductor with line nodes, a linear T dependence of $\lambda(T)$ would be expected. However, Hirschfeld and Goldenfeld[25] showed that scattering would lead to a transition from a T to a T^2 dependence extending to a crossover temperature $T^{imp}\sim T_{c0}\sqrt{(T_{c0}-T_c)/T_{c0}}$, where T_{c0} is the critical temperature in the ultrapure limit ($T_{c0}=1.5$ K). But T^{imp} is predicted to increase with increased scattering, contrary to the observed dependence.

An alternative model by Koszin and Leggett[26] suggested that nonlocality could also give rise to a T^2 dependence of $\Delta\lambda$ in the presence of line nodes, which could be important if

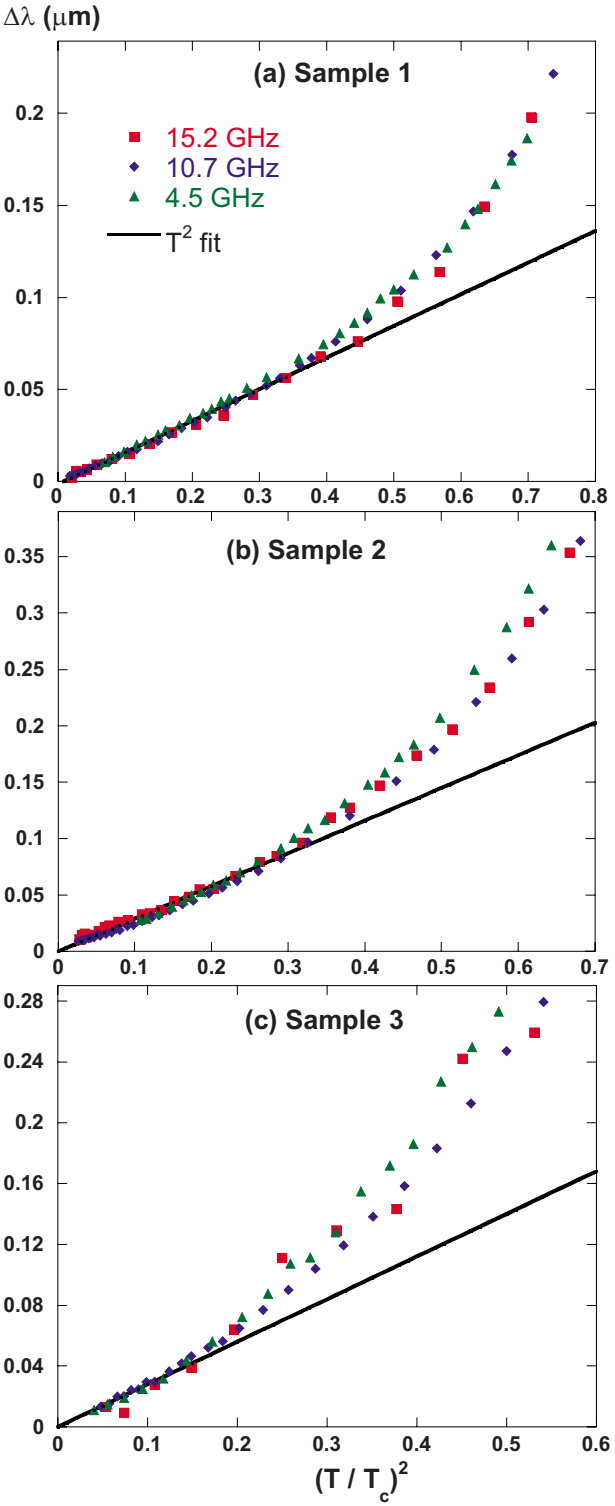

FIG. 3. (Color online) The temperature dependence of $\Delta\lambda$ plotted against $(T/T_c)^2$ for each sample.

$SrRuO_4$ had a nonchiral gap parameter with line nodes. This arises because, for currents flowing in the *ab* plane, $\kappa_c\sim\lambda_{ab}/\xi_{ab}\sim1-2$ so that Sr_2RuO_4 is only just within the local London limit. The presence of nodes or strong anisotropy could therefore lead to an increase in the coherence length along certain directions, so that nonlocal effects become important. Kosztin and Leggett showed that this can

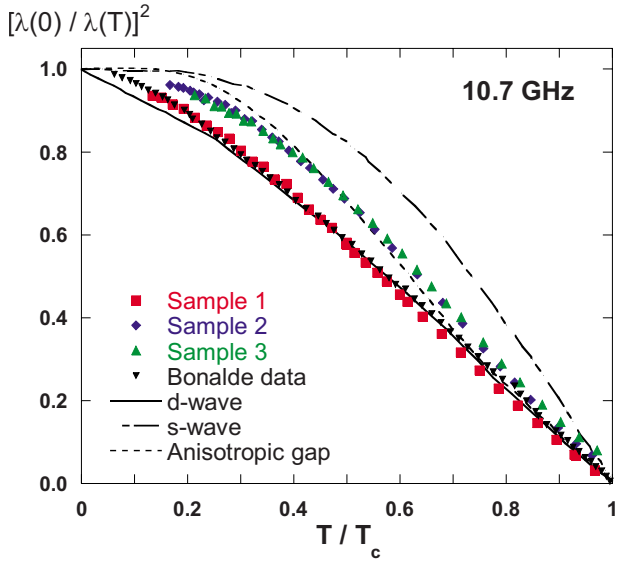

FIG. 4. (Color online) $[\lambda(0)/\lambda(T)]^2$ $[=f(T)]$ vs T/T_c for each sample at 10.7 GHz.

lead to a T^2 dependence of $\lambda(T)$ up to a cross-over temperature $T^{NL} \sim (\xi_0/\lambda_0)\Delta_0$. We would anticipate similar behavior for any superconductor with nodes in the energy gap.

Using the above expression and an estimate of ξ_0 from measurements of the upper critical field B_{c2}, we obtained values for the predicted cross-over temperature of ~1.2, 0.7 and 0.4 K for samples 1, 2, and 3, respectively. Although these temperatures are slightly above those observed, they are in qualitative agreement with the predicted values suggesting that nonlocal effects may well be important. No linear temperature dependence is observed at higher temperatures, but this may be masked by thermal excitations across the gap, particularly if the energy gap on the α and β bands is rather small.

C. Microwave conductivity

We now consider the frequency and purity dependence of the normalized real and imaginary components of the microwave conductivity as a function of reduced temperature derived from the surface impedance measurements. We first consider the imaginary component of the microwave conductivity, which is directly related to the penetration depth and superconducting fraction $f(T)=[\lambda(0)/\lambda(T)]^2=\sigma_2(T)/\sigma_2(T)$ plotted in Fig. 4, for measurements at 10.7 GHz. Measurements at other frequencies showed an almost indistinguishable temperature dependence. These measurements were relatively insensitive to the small corrections made to the measured values of $X_s(T)$ to ensure that $\lambda(0)$ was independent of frequency. Also plotted are the lower frequency measurements of Bonalde *et al.*[23] for a pure sample (T_c=1.39 K) and theoretical predictions for *s*, *d* wave, and an anisotropic gap model with $\Delta_{min}/\Delta_{max}=0.25$, corresponding to the maximum anisotropy inferred from in-plane field-orientated specific-heat measurements.[27]

The microwave measurements for the pure sample are in close agreement with Bonalde's tunnel-diode measurements

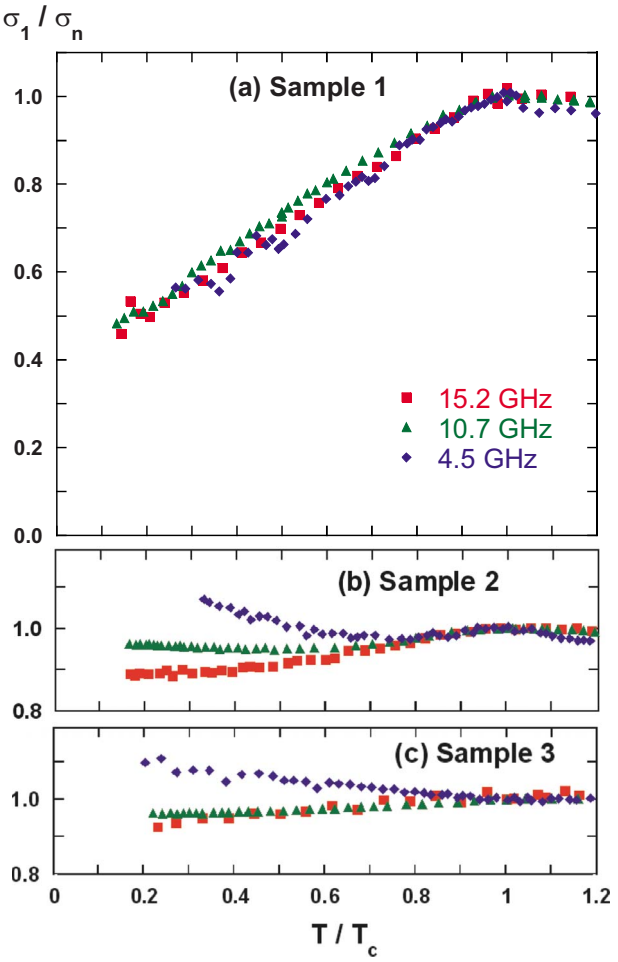

FIG. 5. (Color online) σ_1/σ_n vs T/T_c for each sample (note reduced *y*-axis for sample 2 and 3).

at 28 MHz and exhibit a strong temperature dependence at low temperatures not dissimilar to that of a *d*-wave superconductor, which, in this case, could be attributed to a small gap on the α and β bands. In contrast to Bonalde, we observe slight deviations from a monotonic slope, consistent with multi or anisotropic gap behavior.

For the less pure samples, we observe a much flatter variation at low temperatures, consistent with the suppression by impurity scattering of the effects of superconductivity with nodes or high anisotropy. The suppression of nodal or high anisotropic behavior for the less pure samples may be due to the suppression of superconductivity on the α and β bands, as predicted in the second scenario fitting of Z_s. However, the temperature dependence is still considerably larger than would be expected for an isotropic superconductor. The low-temperature slope is also larger than expected for a superconductor with the largest anisotropy inferred from field-orientated specific heat measurements. This suggests that impurity scattering does not completely suppress the effects of nodes or high anisotropy.

The corresponding plots for σ_1/σ_n, normalized at T_c, are shown in Figs. 5(a)–5(c). It should be noted that the shape of the derived σ_1/σ_n curves are very sensitive to the values of ρ_0 and $\lambda(0)$ used to calculate them. Therefore the data is not

as reliable as the $[\lambda(0)/\lambda(T)]^2$ curves, which are very robust with respect to these parameters.

There is no evidence for coherence peaks for any of the samples, consistent with NMR results.[28] In the case of sample 1, the σ_1/σ_n curves are frequency independent and extrapolate at low temperature to ~0.4, consistent with the RMNF value obtained from Z_{sn} fits. However, for samples 2 and 3 we observe frequency and temperature deviations, particularly at the lowest frequency measured. Such variations may be related to the slight deviations of the experimental results for X_s from those predicted from our empirical two-fluid model, illustrated in Fig. 1. The experimental or theoretical origin of these differences is yet to be explained

IV. SUMMARY

Measurements of the real and imaginary components of the microwave surface impedance at 4.5, 10.7, and 15.2 GHz of the proposed *p*-wave superconductor Sr_2RuO_4 have been made, as a function of temperature and purity.

At low temperatures, all samples exhibited significant microwave losses attributed to a residual fraction of unpaired charge carriers, which increases with increasing amounts of impurity scattering. The measurements can be described by an empirical two-fluid model allowing for different charge carrier properties on the α, β, and γ bands.

For the purest crystal with $T_c \sim 1.40$ K, the measurements could be equally well described in a first case scenario with 42% of the charge carriers remaining unpaired or in a second case scenario with a fully gapped γ band with $63 \pm 17\%$ of the α and β charge carriers remaining unpaired. For the two less pure samples with T_cs of 1.24 and 0.74 K, the measurements could be equally well described with 86% and 96% of the charge carriers remaining unpaired or with superconductivity fully depressed on the α and β bands and partially suppressed on the γ band with residual microwave normal fractions of 56 and 80%, respectively. The measurements could not be described in a scenario in which superconductivity was only suppressed on the α and β bands for the two less pure sample. This is consistent with the continuing depression of the bulk T_c with increased impurity scattering.

Values of $\lambda(0)$ increasing with decreasing purity of 1600 ± 50 Å, $3,000 \pm 50$ Å, and $4,100 \pm 50$ Å for three samples with T_cs of 1.40, 1.24, and 0.74 K were derived from measurements extrapolated to zero temperature.

At low temperatures, $\lambda(T)$ initially increases as T^2 up to a cross-over temperatures that decreased with decreasing purity, as predicted by Koszin and Leggett[26] for superconductors with nodes in the gap parameter, when nonlocal superconducting properties become important. This might then signify nonchiral *p*-wave pairing, though no microscopic theory for such an effect has, to the best of our knowledge, addressed this problem for a *p*-wave superconductor.

The derived temperature dependence of the superfluid fraction $[\lambda(0)/\lambda(T)]^2$ at low temperatures is markedly dependent on purity, consistent with a small superconducting gap on the α and β bands, which is rapidly suppressed by impurity scattering.

For all samples, the superconducting properties described by the generalized two-fluid model were consistent with the quasiparticle lifetimes remaining largely unchanged on entering the superconducting state. This leads to values of the real part of the microwave conductivity decreasing monotonically to the RMNF value at low temperatures. However, at the lowest frequency, the less pure samples exhibit an unexpected frequency and temperature dependence, which reflects deviations of measured X_s from the predictions of the empirical model.

ACKNOWLEDGMENTS

This research has been funded by the EPSRC of the United Kingdom. We are grateful to E.M. Forgan for many helpful discussions and valuable comments.

[1] A. P. Mackenzie and Y. Maeno, Rev. Mod. Phys. **75**, 657 (2003).
[2] Y. Maeno *et al.*, Nature (London) **372**, 532 (1994).
[3] T. M. Rice and M. Sigrist, J. Phys.: Condens. Matter **7**, L643 (1995).
[4] J. F. Annett, G. Litak, B. L. Gyorffy, and K. I. Wysokinski, Phys. Rev. B **73**, 134501 (2006).
[5] C. Kallin, and A. J. Berlinsky, J. Phys.: Conden. Matter **21**, 164210 (2009).
[6] Z. K. Deguchi and Y. Maeno, J. Phys. Soc. Jpn. **73**, 1313 (2004).
[7] T. Nomura and K. Yamada, J. Phys. Soc. Jpn. **71**, 404 (2002).
[8] A. P. Mackenzie, R. K. W. Haselwimmer, A. W. Tyler, G. G. Lonzarich, Y. Mori, S. Nishizaki, and Y. Maeno, Phys. Rev. Lett. **80**, 161 (1998).
[9] Z. Q. Mao, Y. Mori, and Y. Maeno, Phys. Rev. B **60**, 610 (1999).
[10] A. J. Millis, S. Sachdev, and C. M. Varma, Phys. Rev. B **37**, 4975 (1988).
[11] S. Nishizaki, Y. Maeno, and Z. Mao, J. Low Temp. Phys. **117**, 1581 (1999).
[12] K. Ishida *et al.*, Nature (London) **396**, 658 (1998).
[13] K. Ishida, H. Mukuda, Y. Kitaoka, Z. Q. Mao, Y. Mori, and Y. Maeno, Phys. Rev. Lett. **84**, 5387 (2000).
[14] R. J. Ormeno, M. A. Hein, T. L. Barraclough, A. Sibley, C. E. Gough, Z. Q. Mao, S. Nishizaki, and Y. Maeno, Phys. Rev. B **74**, 092504 (2006).
[15] D. A. Bonn, P. Dosanjh, R. Liang, and W. N. Hardy, Phys. Rev. Lett. **68**, 2390 (1992).
[16] W. A. Huttema, B. Morgan, P. J. Turner, W. N. Hardy, X. Zhou, D. A. Bonn, R. Liang, and D. M. Broun, Rev. Sci. Instrum. **77**, 023901 (2006).
[17] S. Sridhar and W. L. Kennedy, Rev. Sci. Instrum. **59**, 531 (1988).
[18] Y. Maeno *et al.*, J. Phys. Soc. Jpn. **66**, 1405 (1997).
[19] A. P. Mackenzie, S. R. Julian, A. J. Diver, G. J. McMullan, M. P. Ray, G. G. Lonzarich, Y. Maeno, S. Nishizaki, and T. Fujita,

Phys. Rev. Lett. **76**, 3786 (1996).
[20] M. Tinkham, *Introduction to Superconductivity* (McGraw-Hill, Inc., New York,1996).
[21] J. R. Waldram, P. Theopistou, A. Porch, and H. M. Cheah, Phys. Rev. B **55**, 3222 (1997).
[22] W. N. Hardy, D. A. Bonn, D. C. Morgan, R. Liang, and K. Zhang, Phys. Rev. Lett. **70**, 3999 (1993).
[23] I. Bonalde, B. D. Yanoff, M. B. Salamon, D. J. Van Harlingen, E. M. E. Chia, Z. Q. Mao, and Y. Maeno, Phys. Rev. Lett. **85**, 4775 (2000).
[24] K. Miyake and O. Narikiyo, Phys. Rev. Lett. **83**, 1423 (1999).
[25] P. J. Hirschfeld and N. Goldenfeld, Phys. Rev. B **48**, 4219 (1993).
[26] I. Kosztin and A. J. Leggett, Phys. Rev. Lett. **79**, 135 (1997).
[27] K. Deguchi, Z. Q. Mao, H. Yaguchi, and Y. Maeno, Phys. Rev. Lett. **92**, 047002 (2004).
[28] K. Ishida, Y. Kitaoka, K. Asayama, S. Ikeda, S. Nishizaki, Y. Maeno, K. Yoshida, and T. Fujita, Phys. Rev. B **56**, R505 (1997).